Available online at www.sciencedirect.com
SCIENCE DIRECT®
Journal of Molecular Graphics and Modelling 24 (2005) 203–212
Journal of Molecular Graphics and Modelling
www.elsevier.com/locate/JMGM

Insights into the induced fit mechanism in antithrombin–heparin interaction using molecular dynamics simulations

Hugo Verli, Jorge A. Guimarães *

Centro de Biotecnologia, Universidade Federal do Rio Grande do Sul, Av. Bento Gonçalves, 9500, CP 15005, Porto Alegre 91500-970, RS, Brazil

Received 18 July 2005; accepted 22 July 2005
Available online 16 September 2005

Abstract

Heparin was isolated in the beginning of the 20th century and until today remains as one of the most important drugs able to interfere with the haemostatic process. Due to the side effects produced by heparin therapy, new promising drugs have been developed, as the synthetic pentasaccharide (synthetically derived from the sequence GlcN-GlcA-GlcN-IdoA-GlcN). The anticoagulant activity of this compound is based on potentiation of antithrombin (AT) inhibitory activity upon serine proteinases of clotting cascade, a mechanism based on the conformational modification of AT. In this context, we present here a molecular dynamics (MD) study of the interaction between the synthetic pentasaccharide and AT. The obtained data correctly predicted an induced fit mechanism in AT–pentasaccharide interaction, showing a solvent-exposed P1 residue instead of a hided conformation. Also, the specific contribution of important amino acid residues to the overall process was also characterized, both in $^{2}S_{0}$ and $^{1}C_{4}$ conformations of IdoA residue, suggesting that there is no conformational requirement to the interaction of this residue with AT. Altogether, the results show that MD simulations could be used to characterize and quantify the interaction of synthetic compounds with AT, predicting its specific capacity to induce conformational changes in AT structure. Thus, MD simulations of heparin (and heparin-derived)–AT interactions are proposed here as a powerful tool to assist and support drug design of new antithrombotic agents.

Keywords: Carbohydrate; Molecular dynamics; Serpin; Antithrombin; Synthetic pentasaccharide; Heparin; Induced fit

1. Introduction

Heparin was identified and then isolated in 1916 from a preparation of dog liver, being the first compound used clinically as anticoagulant and antithrombotic agent [1]. It is mainly composed of hexasaccharide units containing iduronic acid (IdoA) 2-sulfate, glucosamine (GlcN) 2,6-disulfate, and non-sulfated glucuronic acid (GlcA) [2], whereas small variations may occur among heparins from different sources [1]. Until today, heparin remains as one of the most important and efficient antithrombotic therapeutic agents because of its ability to interfere with the haemostatic process. Most recently, new promising drugs, as the synthetic pentasaccharide (Fig. 1), has been approved for clinical use [3].

The anticoagulant activity of heparin and other negatively charged glycosaminoglycans is due to the activation of a plasma protein called antithrombin (AT). This protein belongs to the serpin (serine proteinase inhibitors) protein family and is responsible for the inhibition of physiologically active plasma serine proteinases like fIIa and fXa. The activation of AT by heparin is due to two main mechanistic components: (1) a bridging interaction through which the linear heparin molecule binds simultaneously to both AT and proteinase; and (2) a conformational change-based mechanism in which the heparin binding induces AT conformational changes, increasing its reactivity towards the target proteinase [4].

The reactive bond that interacts with the active site of target proteinases lies on a loop denoted as reactive center loop (RCL), which comprises in AT structure the sequence between residues Asn376 and Arg393, i.e. P17 and P1,

* Corresponding author. Tel.: +55 51 3316 6068; fax: +55 51 3316 7309.
E-mail address: guimar@cbiot.ufrgs.br (J.A. Guimarães).

1093-3263/$ – see front matter © 2005 Elsevier Inc. All rights reserved.
doi:10.1016/j.jmgm.2005.07.002

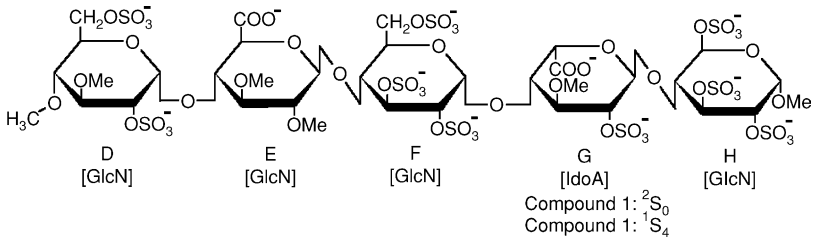

Fig. 1. Structure of the synthetic pentasaccharide compounds 1 ($^2S_0$) and 2 ($^1C_4$). Concerning the nomenclature used for each carbohydrate residue, see Section 2.

respectively, using the notation of Schechter and Berger [5]. In the native conformation, the RCL lies outside the tertiary core of the serpin main structure, i.e. in a solvent-exposed environment. However, in crystallographic structures this region is often involved in protein–protein contacts [6–8], already reported as a necessary event in order to support the observation of RCL coordinates in the final three-dimensional structure [9].

Efforts to elucidate the heparin recognition by AT–proteinase complex at the atomic level have faced difficulties in structure determination and dynamics regarding the participation of polysaccharides in general [10]. Just recently a work of Li et al. [11] presented the crystallographic structure of the complex between heparin, AT and thrombin. In this context, we have previously presented a reliable molecular dynamics (MD) protocol to simulate heparin in physiological conditions, e.g. salt concentration and explicit water representation [12]. The use of this MD methodology allowed simulation of carbohydrates in their natural environment, describing its dynamic properties with a reasonable level of accuracy.

The aim of this work is to evaluate the dynamics of AT–heparin complex, using the synthetic pentasaccharide (compound 1, Fig. 1) as a model. We also studied the influence of IdoA conformational equilibrium in heparin recognition. To this purpose, 8.0 ns MD simulation of both unbound AT and AT bounded to compound 1 has been performed. The results of these simulations are compared to crystallographic and mutagenesis data, concerning the AT–heparin system, to validate the obtained data. Finally, a MD-based scheme for heparin conformational modulation of AT is proposed, in which the IdoA conformation is not a requirement to formation of the AT–heparin complex. Also, several of the AT conformational modifications induced by heparin were well predicted, as the side chain conformation of Arg393 (P1) being solvent-exposed instead of solvent hided, apparently due to crystallographic contacts. This is, to our knowledge, the first report describing such mechanisms using MD simulations.

2. Methods

2.1. Nomenclature and software

The recommendations and symbols of nomenclature as proposed by IUPAC [13] were used. The relative orientation of a pair of contiguous sugar residues (e.g. iduronic acid, glucosamine and/or glucuronic acid) is described by two torsional angles at the glycosidic linkage, denoted ϕ and ψ. For a (1 → 4) linkage the definitions become those shown in Eqs. (1) and (2):

$$\phi = \text{O5}-\text{C1}-\text{O1}-\text{C4}' \quad (1)$$

$$\psi = \text{C1}-\text{O1}-\text{C4}'-\text{C5}' \quad (2)$$

The topologies of compounds 1 and 2 were generated with the PRODRG program [14], manipulation of structures was performed with MOLDEN [15], VMD [16], and MolMol [17] programs, the homology modeling was performed with the Swiss-PDB Viewer [18], and all the MD calculations and analysis were performed using the GROMACS simulation suite and force field [19,20].

Due to structural similarities between the synthetic pentasaccharide and heparin, the residues D, E, F, G, and H were named according to the heparin residues GlcN, GlcA, GlcN, IdoA, and GlcN, respectively. This nomenclature was chosen in order to facilitate further structure–activity relationships. The main differences between the residues of the synthetic polysaccharide and the natural polysaccharide are the methoxylation of hydroxyl groups and the substitution of sulfonamide groups by sulfate groups.

2.2. Topology construction

The topologies for compounds 1 and 2 were built as previously described [12]. The pentasaccharide structure in 1E03 PDB code, presenting its IdoA residue in a $^2S_0$ conformation, was submitted to the PRODRG site [14], and the initial geometry and topologies were retrieved, corresponding to compound 1.

The two conformational states of IdoA residue ($^2S_0$ and $^1C_4$) were defined by the addition of improper dihedral angles in the respective topology files. These angles intend to fix the IdoA geometry in chair or skew-boat conformations, so the same topology obtained for compound 1 could be used for compound 2 just by changing the improper dihedral values (for details see [12]). The atomic charges were obtained from a previous work of our group [12].

2.3. Structure refinement and molecular simulations

The AT–pentasaccharide complex was retrieved from PDB under code 1E03 [21]. The gap between positions 28 and 37 was fulfilled by means of homology modeling using the Swiss-Pdb Viewer program [18]. Based on this structure the unbound AT and the complexes formed between AT and compounds 1 and 2 were built, comprising three systems simulated for 8.0 ns each one. In addition, the two compounds were isolated from AT comprising two systems simulated for 2.0 ns each one. These structures were solvated in a rectangular box using periodic boundary conditions and SPC/E water model [22]. Counter ions (Na^+) were added to neutralize the system. The MD protocol employed was based on previous MD studies [23], as described [12,24]. The Lincs and Settle methods [25,26] were applied to constrain covalent bond lengths, allowing an integration step of 2fs after an initial energy minimization using Steepest Descents algorithm. Electrostatic interactions were calculated with Particle Mesh Ewald method [27]. Temperature and pressure were kept constant separately by coupling the protein, carbohydrate, ions, and solvent to external temperature and pressure baths with coupling constants of $\tau = 0.1$ and 0.5 ps [28], respectively. The dielectric constant was treated as $\varepsilon = 1$, and the reference temperature was adjusted to 310 K. The systems were heated slowly from 50 to 310 K, in steps of 5 ps, each one increasing the reference temperature by 50 K. To determine if a hydrogen bond exists, a geometrical criterion was used, i.e. $r \leq 0.35$ nm (donor–acceptor distance) and $\alpha \geq 120^0$ (donor–hydrogen–acceptor angle) [20]. Data concerning the structure of compounds 1 and 2 (i.e. glycosidic linkage) and interaction energies were obtained by averaging the property over the entire simulation (8.0 ns for the complex simulations and 2.0 ns for the uncomplexed ligands).

3. Results and discussion

3.1. Simulation systems

Three simulations, each one 8.0 ns long, were performed including the unbound AT and the complexes of AT with compounds 1 and 2 (Fig. 1). Compound 1 corresponds to the synthetic pentasaccharide in its crystallographic conformation, with the IdoA residue in a $^2S_0$ twist-boat conformation while compound 2, with the same pentasaccharide structure, had its IdoA residue changed to a $^1C_4$ chair conformation (see Section 2 for details). The AT structure in its inhibitory form was retrieved from PDB code 1E03. The simulation systems comprised about 47,000 atoms, including counter ions and solvent molecules. Simulations of 2.0 ns were also performed including only solvent, compound 1 or compound 2, and counter ions, without the AT molecule.

3.2. Simulation stability

To monitor the progress of the performed simulations we evaluated the root mean square deviation (RMSD) of the simulated complexes from the crystallographic structure as a function of time. As can be observed in Fig. 2, all simulations were stable during the performed time scale,

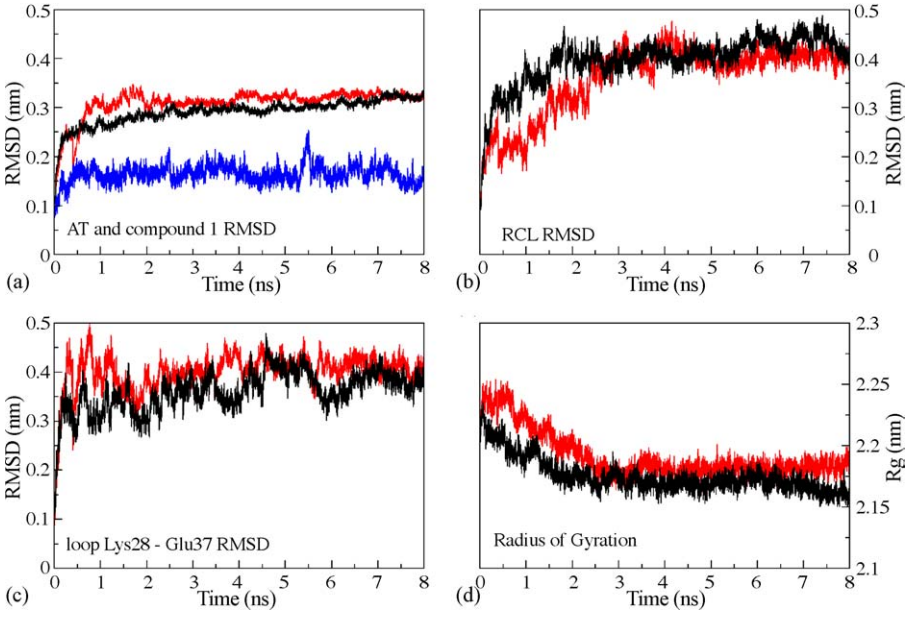

Fig. 2. All-atom RMSD from crystal structure and radius of gyration for unbound AT (red) and AT–compound 1 complex (black). (a) RMSD for bounded AT, for unbounded AT and for compound 1 (blue); (b) RMSD for the RCL sequence (comprising residues Asn376–Arg393, i.e. P17–P1); (c) RMSD for the loop-comprising residues Lys28–Glu37; and (d) radius of gyration.

with an average RMSD for the entire protein of about 0.3 nm for both complexed and uncomplexed AT. However, the unbound AT (red curve in Fig. 2a) presents a higher RMSD when compared to AT–compound 1 complex (black curve in Fig. 2a) for almost all the simulation time. This profile is probably due to the starting structure used in the simulations, i.e. the crystallographic complex between AT and compound 1 (1E03). Instead of using an unbound form of AT to simulate its free state, we decided to use the 1E03 structure, with the removal of compound 1. Doing so, we could observe the behavior of the conformational modifications induced in AT by compound 1 in its absence and in the presence of water. Therefore, in absence of compound 1 the forces that induce and stabilize these conformational changes are removed, so creating instabilities in AT solution simulations. Also a low RMSD value can be observed for compound 1 when complexed to AT (blue curve in Fig. 2a), as a possible consequence of the high affinity of polysulfated polysaccharides, such as compound 1, showing to be able to make specific complexes with AT.

The RMSD of the loop between positions 28 and 37 is presented in Fig. 2c. It seems that the high flexibility that this loop presents is indicative of its absence in serpin crystal structures, i.e. the diversity of conformations in solution could be kept in the crystal, creating a region of the crystalline cell with poor organization (see further).

As observed for the loop 28–37, the RCL also shows high flexibility (Fig. 2b). In this case, a slope can be clearly identified in the first 2.5 ns for unbounded AT (red curve in Fig. 2b) and in the first 2.0 ns for AT complexed with compound 1 (black curve in Fig. 2b). After this initial slope a stable profile is observed, with no clear distinction between the complexed and uncomplexed forms of AT. These slopes are highly correlated with the decreasing of radius of gyration in the beginning of simulation (Fig. 2d), suggesting that a possible compacting process of the protein moiety is part of AT equilibration in solution.

3.3. Structural fluctuations of antithrombin

In order to assess the relative mobility of different regions of AT we analyzed the root mean square fluctuations (RMSF) as a function of residue number and time (Fig. 3) for unbound AT and AT–compound 1 complex. The analysis of the RMSF variation as a function of time, instead of a total average analysis, indicated some important features. As seen in Fig. 2, the equilibration of the simulated systems is markedly distinct over different regions of AT. The regions defined by the RCL and by the N-terminal loop, comprised by residues Lys28 and Glu37, present the slowest equilibration of the entire protein. While the RCL keeps a high flexibility over the entire trajectory, the loop 28–37 accommodates in solution after 2 ns or 3 ns, depending on the AT complexation state. Therefore, this equilibration period of 2–3 ns represents the searching of the loop for its solution conformation. However, it is interesting to observe that the loop 28–37 presents a lower flexibility in the complexed AT compared to the unbound AT. At the same time the RCL flexibility is greater in the complexed form of AT than in the free protein. While these differences could be associated to the degree of conformational sampling of the MD instead of a solution behavior, they are observed in more than 4.0 ns (the second half of the simulation), indicating the consistence of the simulation data. In this context, we consider the possibility that the mentioned RMSF profile is due to compound 1 effects over AT: (1) stabilizing the sequence comprised between Lys28 and Glu37; and (2) increasing the flexibility of the RCL. In other words, the conformational modifications expected to be

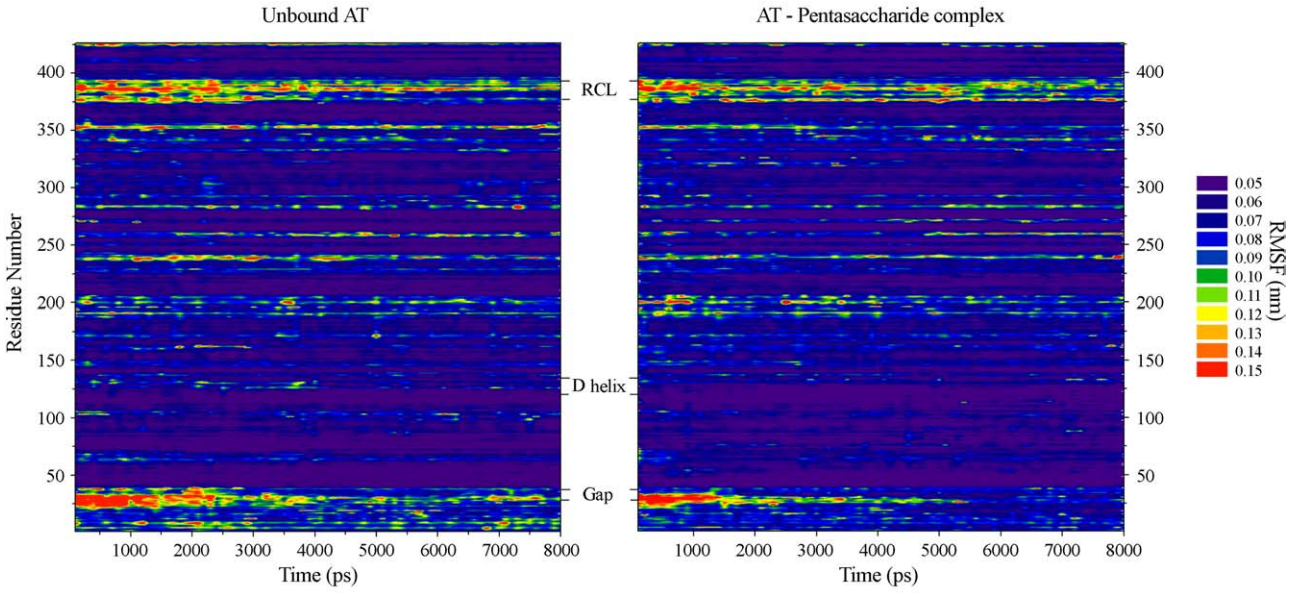

Fig. 3. RMSF as a function of both residue number and time for unbound AT and AT–compound 1 complex. The regions corresponding to the loop-comprising residues Lys28–Glu37 (Gap), D-helix and the reactive center loop (RCL) are also presented.

induced in AT by compound 1, which results in the profound potentiating effect of its inhibitory activity, could be observed and predicted by MD simulations.

3.4. Structural fluctuations of the polysaccharide moiety

In order to test the AT capabilities to induce conformational modifications in heparin, as previously suggested [29], we performed MD simulations of compounds 1 and 2 in solution, in absence of the protein moiety.

The structure and flexibility of the simulated carbohydrates were evaluated on the basis of the glycosidic linkage variation over the MD trajectory, as already reported [12]. The average dihedral angles of the glycosidic linkage for compounds 1 and 2 in solution or complexed with AT are presented in Table 1. For comparison, the reference values for ϕ and ψ dihedral angles as obtained by NMR [30] and crystallography [21] studies were also presented.

With respect to the pentasaccharide simulations, it must be observed that, so far, there is no three-dimensional structure determined by experimental methods evidencing the solution geometry of GlcN → GlcA and GlcA → GlcN dihedral angles inside heparin or even any other polysaccharide molecule. The heparin structure previously reported concerns to a dodecasaccharide [30] composed exclusively by GlcN and IdoA residues, without GlcA. The only reference available to the heparin GlcN → GlcA and GlcA → GlcN dihedral angles is the crystallographic complex between compound 1 and AT [21]. This structure, however, may not correctly represent the heparin solution structure for two major reasons: (1) the synthetic pentasaccharide could have suffered conformational modifications as consequence of an induced fit mechanism; and (2) the synthetic pentasaccharide presents several structural modifications regarded to heparin, e.g. the substitution of hydroxyl by methoxyl groups and the substitution of sulfonamide by sulfate groups (Fig. 1). Even considering that these chemical modifications did not impair the anticoagulant activity of the compounds, such substitutions are possibly inducing conformational modifications in the pentasaccharide compared to heparin.

As shown in Table 1, the MD simulations of compounds 1 and 2 in solution and complexed with AT were well correlated with the reference values obtained from NMR [30] and X-ray crystallography (Table 1) [21]. However, the dynamics of some of the glycosidic linkages have considerable differences between free and complexed compounds, suggesting that heparin-derived saccharides displaying anticoagulant activity interacts with AT by means of an induced fit mechanism. For instance with both compounds 1 and 2, the GlcN → IdoA ϕ angle change about 30° when complexed with AT. Significant alterations in the ligand–protein complex can be also observed for other angles: GlcN → GlcA ψ (∼20° for compound 1) and GlcN → IdoA ψ (∼20° for compounds 1 and 2). It should be noted that the conformation of IdoA appears not to interfere with the ligand conformational change once interacting with the target protein, since both compounds 1 and 2 can achieve the same bounded conformation.

These data may indicate that the overall geometry of the polysaccharide, as well as the IdoA geometry, is not a necessary prerequisite for AT activation, being the crystallization of its $^2S_0$ form in the AT–pentasaccharide complex [21] due to a larger population of the skew-boat conformation over the chair conformation instead of the preference of AT to select such a conformation. In this way, the ligand plasticity seems to play a crucial role in inducing the required AT conformation in order to allow the protein to exert its potent anticlotting activity.

3.5. Ligand-receptor recognition

An understanding of those chemical forces which can drive the binding of heparin-derived compounds to AT could

Table 1
Glycosidic linkage average of dihedral angles observed upon MD simulation of compounds 1 and 2 alone or complexed with AT

Dihedral angles[a]	NMR[b,c]	NMR[b,d]	1E03[e]	Average dihedral (°)[a,f]			
				1[g]	2[g]	1[h]	2[h]
GlcN → GlcA (ϕ)		–	96.9	89.5	85.8	77.9	77.3
GlcN → GlcA (ψ)		–	−153.7	−129.9	−135.6	−149.2	−149.4
GlcA → GlcN (ϕ)		–	−72.5	−85.1	−87.3	−83.9	−87.7
GlcA → GlcN (ψ)		–	−116.8	−131.4	−128.9	−120.3	−117.2
GlcN → IdoA (ϕ)	108.6	78.7	45.7	89.6	89.6	59.4	48.2
GlcN → IdoA (ψ)	−157.5	−149.9	−151.1	−126.9	−130.5	−144.4	−149.2
IdoA → GlcN (ϕ)	−55.4	−77.1	−78.1	−77.7	−76.8	−63.3	−72.1
IdoA → GlcN (ψ)	−107.4	−110.1	−92.9	−116.5	−118.2	−108.8	−105.3

[a] See Section 2 for details.
[b] Data obtained from PDB code 1HPN [30].
[c] IdoA residues in $^2S_0$ conformation.
[d] IdoA residues in $^1C_4$ conformation.
[e] Data obtained from PDB code 1E03 [21].
[f] Standard deviation is approximately ±15° for all values.
[g] Molecules in solution.
[h] Complex with AT.

Table 2
Interaction energy analysis between AT and the simulated polysaccharides

AT residues[a]	Average interaction energy (kJ/mol)	
	Compound 1	Compound 2
Lys11	−101.5 ± 35.8	−92.9 ± 31.4
Arg13	−77.9 ± 41.9	−102.7 ± 30.1
Thr44	−43.4 ± 10.6	−52.3 ± 15.3
Asn45	−108.5 ± 13.9	−117.3 ± 12.1
Arg46	−19.5 ± 9.8	−37.7 ± 23.4
Arg47	−147.5 ± 12.2	−144.1 ± 10.9
Glu113	−45.5 ± 8.3	−46.6 ± 7.8
Lys114	−211.6 ± 9.8	−225.3 ± 11.9
Lys125	−27.4 ± 23.9	−63.5 ± 40.2
Arg129	−25.2 ± 20.8	−43.0 ± 10.2
Arg132	−3.1 ± 7.2	−8.3 ± 11.7
Lys133	−0.1 ± 0.4	−0.8 ± 1.1
Lys136	0.0 ± 0.0	0.0 ± 0.0
Total	−965.7 ± 72.5	−1124.0 ± 61.4

[a] The selected amino acids correspond to approximately 80% of the total interaction energy between the simulated compounds and AT.

aid in the design of new antithrombotic compounds based on the conformation-induced mechanism of AT activation. In this context we evaluated the main interactions contributing to compound 1–AT complex. As shown in Table 2 some of these interactions ranged from −100 to −200 kJ/mol, approximately, confirming the recognized predominance of electrostatic contributions to the heparin–AT interaction. In general these high energy electrostatic interactions include several hydrogen bonds with different acceptors. For example, Arg47 makes hydrogen bonds with two distinct oxygen atoms from 2-O-sulfate group from residue H (GlcN), while performing a hydrogen bond with the carboxylate group of residue G (IdoA, Fig. 4). In the same way, Lys114 also performs several interactions, in a total of five hydrogen bonds with different acceptor atoms of compound 1 (Fig. 4). Altogether compound 1 performs an average of 15.9 ± 2.7 hydrogen bonds over the 8.0 ns of simulation. As this value is an average, it hides values ranging from 7 to 30 hydrogen bonds as the interactions between ligand and receptor fluctuate. This complex mosaic of intermolecular interactions can be simplified by means of interaction energy analysis, indicating the relative contribution of each residue as shown in Table 2. Such kind of information has important implications in the structure-based design of new antithrombotic compounds, indicating the particular contribution of each amino acid residue of AT and its possible relation to conformational modification of the interacting polysaccharide.

This is, to our knowledge, the first attempt to quantitatively determine the contribution of each one of the AT amino acid residues in their interactions with heparin-derived compounds. Our results are plentifully supported by other works reporting qualitative data on this subject, including X-ray crystallography [21] and mutagenesis studies [32–36]. Since the accuracy of a method can be judged by how well it reproduces known quantities [37,38], the obtained energies for the interactions between AT and compound 1 corroborates the validity of the performed simulations in describe the AT–heparin system.

3.6. Reactive center loop dynamics

The structures of both I- and L-AT (i.e. inhibitory and latent AT, respectively) co-crystallize as a dimmer in which the I-AT RCL is partially inserted in the structure of L-AT [21,39]. This alignment appears to be held by a series of electrostatic interactions and hydrophobic contacts, including residues Glu237–Tyr240, Met251, Tyr260, Leu270, Leu285, Leu316–Val317, His319, Pro321, and Arg406 from L-AT and Glu255, Met315, and Thr386–Arg399 from I-AT, thus comprising almost all the RCL [21]. In this restrained conformation of RCL the P1 residue remains hided from solvent. This seems to represent a particular structural form since in other serpin crystal structures the P1 residue lies in a

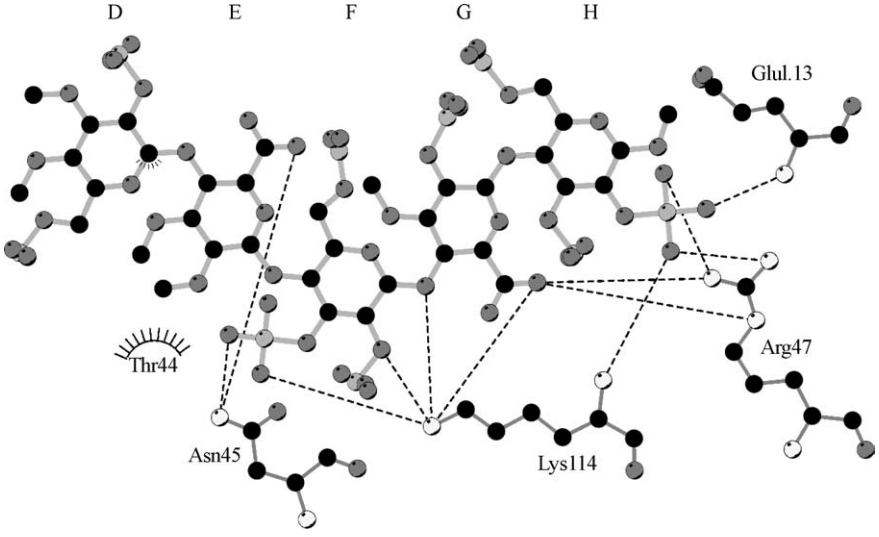

Fig. 4. Ligplot cartoon illustrating compound 1 binding to AT [31].

solvent-exposed manner [40]. What is not clear is whether the interaction with the latent molecule forces the RCL of the active molecule into this conformation or whether its preference for this conformation in solution allows it to co-crystallize with a latent partner [4]. Anyway the orientation of the RCL inserted into the L-AT implies that the side chain of P1 is in an internal orientation that does not allow the full match with the complementary conformation of the active site of target proteases.

In the MD simulations of the present work the I-AT was isolated from the L-AT, so the network of interactions constraining the RCL in the crystallographic structure was eliminated. Instead of the crystallographic interactions new contacts were created upon the addition of solvent, inducing conformational modifications in AT, as indicated by the time-dependent RMSD variation (Fig. 2), the RMSF (Fig. 3) and a visual examination of the simulations for the RCL and the loop-comprising residues Lys28 to Glu37. These motions could be highlighted in Fig. 5a, where the thickness of the sausage plot indicates the extent of protein chain motion. The highest mobility found in loops 28–37 and 376–393 should have important functional implications since the first loop is adjacent to the heparin binding site and the last comprise the recognition sequence for clotting proteases. In fact, a closer look to P1 residue (Fig. 5b) shows a rotation of this residue of almost 90° in reference to crystal structure with consequent exposure of its side chain to solution and to the target proteases, bringing the RCL backbone closer to the AT body and so the radius of gyration reduction in the beginning of the simulations (Fig. 2d). A similar reorientation of P1 was observed in unbound AT and AT complexed to compound 2, indicating that instead of the crystallographic conformation of the RCL be due to its preference in solution it appears to be induced by the interactions with the AT latent molecule in the crystal. Also, it seems that the solvent exposure of Arg393 allows better recognition of AT by target proteinases, an assumption supported by previous works suggesting that (1) the P1 side chain is likely to be solvent accessible [41]; and (2) the natural state of the RCL is disordered, switching between a variety of conformers, readily accessible for insertion into the active site of a target protease [9].

Not only the change in P1 orientation was observed in the MD simulations, but important modifications in AT

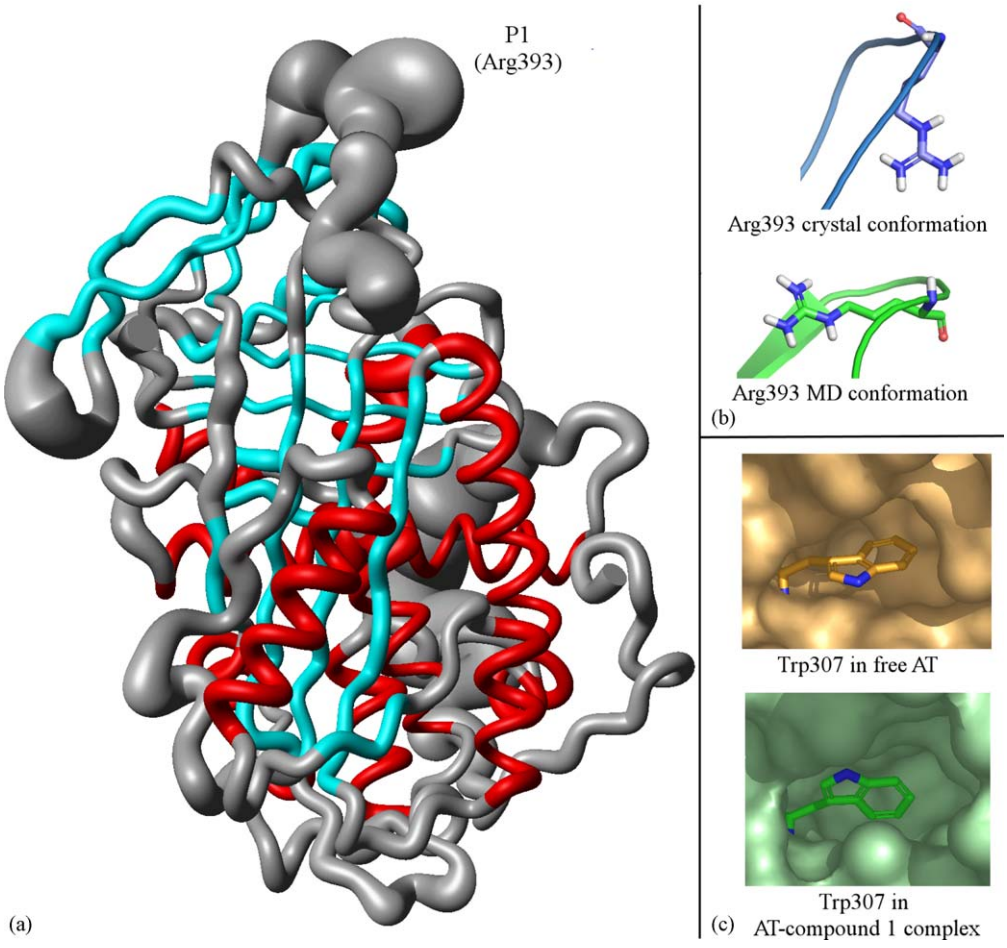

Fig. 5. (a) Sausage plot of AT complexed with compound 1 (omitted in order to clarify the picture). Coils are colored in gray, β-sheets are colored in cyan and α-helices are colored in red; (b) Arg393 in crystal (blue) and MD (green) conformations; and (c) Trp307 in free AT (orange) and in AT–compound 1 complex (green). The figure was prepared by using MolMol [17].

secondary structure were also observed. As previously reported [42,43], the addition of increasing concentrations of heparin to an AT solution induces a progressive increase in its tryptophan fluorescence emission. In agreement with these data, the observation of the Trp307 conformation in the performed simulations indicates a reorientation of its side chain due to formation of AT–compound 1 complex (Fig. 5c). Such tryptophan residue presents an average interaction energy with its surrounding hydrophobic pocket (i.e. Val263, Val269, Ile284, Val295, Leu299, Val303, Leu304, and Leu308) of -91.1 ± 17.3 kJ/mol when in a free form. Due to complexation with compound 1, this interaction energy increases in almost 30 kJ/mol, to -61.7 ± 6.5 kJ/mol, indicating an exposition of Trp307 to solvent and so a change in fluorescence emission. No changes in Trp225 were observed in the performed calculations.

Analysis of the secondary structure of protein using the program DSSP [44] indicated that the D-helix (residues Gln118 to Lys136) decrease its size in MD simulations of unbound AT, but did not in AT complexed to compound 1. Besides the modifications found in the secondary structure of the protein, the PROCHECK program [45] indicated a remarkable quality of the performed simulations, where all the performed checks were found inside the reference values (results not shown).

It was previously proposed that heparin binding causes extension of helix D, which is connected to β-sheet A by a short linker, and that such helix extension causes contraction of β-sheet A and expulsion of the hinge residues P14 and P15 [46]. This process would change the flexibility and conformation of the RCL, which could explain the activation of AT by conformational modifications induced by heparin [47]. So we used other methods in order to confirm the unfolding of this AT-helix in the absence of the synthetic pentasaccharide. In this context the pseudo dihedral angle ξ (the torsion angle between planes defined by four consecutive α-carbon atoms) provides a simplified backbone representation and continues to give information about secondary-structure elements. It could be seen in the plot helical and sheet like regions [48]. The α-helices for instance are marked by a $\xi = 45^{\circ}$. The analysis of the ξ angle is in agreement with the DSSP and PROCHECK analyses, with a reduction in the α-helices character over the first 2.5 ns of simulation (Fig. 6a). Also the ellipticity [49] of the residues His120 to Ala134 (Fig. 6b) indicates progressive lost of the helix character after the residue Arg129. This residue appears to be an inflexion point in the D-helix, the place where it abruptly lost more than 60% of the helix character (Fig. 6b). This is supported by previous data indicating an important role of Arg129 to the induced fit mechanism of heparin activation of AT [36]. This residue performs electrostatic interactions with compounds 1 and 2 and its importance in an induced fit mechanism of AT activation mediated by heparin has been previously suggested [36]. Therefore, the partial unfolding of D-helix, induced by the absence of compound 1 (Fig. 6b), indicates that MD simulations are able to correctly predict the stabilizing effect of heparin over AT D-helix.

Globally, the performed MD simulations make possible a dynamic and temporal connection and interpretation of several experimental data at a molecular level, starting from the polysaccharide–AT complex, with a quantitative description of the relevant interaction for such complex, passing through the induction of D-helix extension and the conformational modification of the carbohydrate moiety, to the increase in RCL flexibility, with emphasis on the structural analysis of the P1 residue exposure. Such profile, observed in solution for P1 conformation, can be considered an alternative view for AT structure in its biological environment when compared to the crystal orientation observed for this residue.

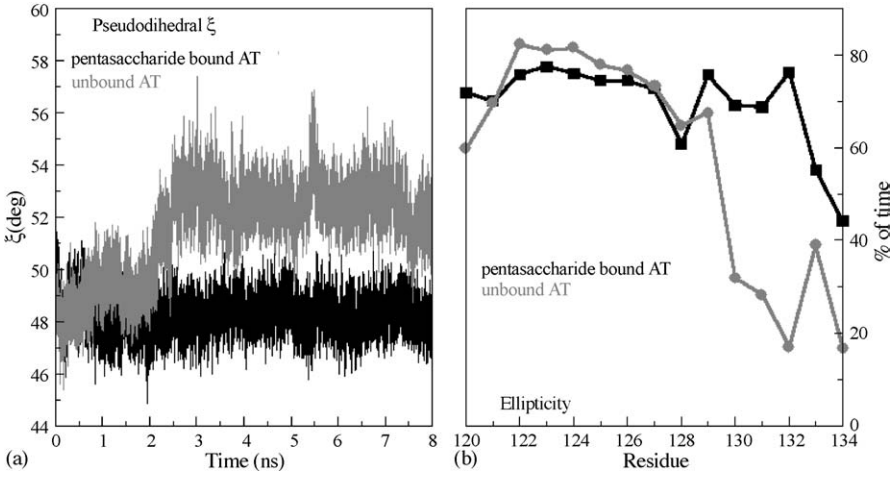

Fig. 6. (a) Pseudo dihedral ξ (i.e. the dihedral formed by 4 consecutive α-carbon atoms $C\alpha_i$, $C\alpha_{i+1}$, $C\alpha_{i+2}$, and $C\alpha_{i+3}$) as a function of time for helix D (residues His120–Ala134) of unbound AT (dark grey) and AT–compound 1 complex (black) [40]; and (b) the ellipticity at 222 nm [49] (percent of time in which the residue presents a helix character) as a function of residue number of unbound AT (dark grey) and AT–compound bound complex (black).

4. Conclusions

The current knowledge concerning antithrombin inhibitory activity and its modulation by heparin has been expanded in the last years by several studies. While these works traced a picture of heparin–AT complex based mainly on rigid X-ray crystallographic structure, mutagenesis and fluorescence studies, the connection of these qualitative information with the solution dynamics of ligand–AT interaction is almost absent, with a minor participation of molecular modeling and MD techniques.

In this context, the present work is the first to describe in the nanosecond time scale the interaction of a heparin analogue with AT using MD simulations. Several detailed conformational changes associated with this process were observed as: (a) formation of additional turns in D-helix in presence of heparin; (b) exposition of P1 to solvent; (c) transmission of conformational changes from D-helix elongation to RCL; and (d) increase in RCL flexibility in the presence of the synthetic pentasaccharide regarded to unbound AT (i.e. AT activation). In addition, the relative contribution of each amino acid residue could be estimated, with a high agreement with previously related mutagenesis and crystallographic data. Our data also suggest that there is no conformational requirement of IdoA to interact with AT, since both skew-boat and chair conformations contribute with similar enthalpy upon its interaction with the target protein.

Together, these data can contribute in the determination of the main requirements for anticoagulant polysaccharides modulating clotting serpins and so to assist in the development of new antithrombotic agents.

Acknowledgements

This work was supported by Conselho Nacional de Desenvolvimento Científico e Tecnológico (CNPq), MCT, Brasília, DF, Brazil; the Coordenação de Aperfeiçoamento de Pessoal de Nível Superior (CAPES), MEC, Brasília, DF, Brazil; and Fundação de Amparo à Pesquisa do Estado do Rio Grande do Sul (FAPERGS), RS, Brazil.

References

[1] H.B. Nader, M.A.S. Pinhal, E.C. Baú, R.A.B. Castro, G.F. Medeiros, S.F. Chavante, E.L. Leite, E.S. Trindade, S.K. Shinjo, H.A.O. Rocha, I.L.S. Tersariol, A. Mendes, C.P. Dietrich, Development of new heparin-like compounds and other antithrombotic drugs and their interaction with vascular endothelial cells, Braz. J. Med. Biol. Res. 34 (2001) 699–709.

[2] M.E. Silva, C.P. Dietrich, Structure of heparin—characterization of products formed from heparin by action f a heparinase and a heparitinase from *Flavobacterium heparinum*, J. Biol. Chem. 250 (1975) 6841–6846.

[3] J. Hirsh, Current anticoagulant therapy-unmet clinical needs, Thromb. Res. 109 (2003) S1–S8.

[4] P.G.W. Gettins, Serpin structure, mechanism, and function, Chem. Rev. 102 (2002) 4751–4803.

[5] I. Schechter, A. Berger, On the size of the active site in proteases. I. Papain, Biochem. Biophys. Res. Commun. 27 (1967) 157–162.

[6] S.-J. Kim, J.-R. Woo, E.J. Seo, M.-H. Yu, S.-E. Ryu, A 2.1 Å resolution structure of an uncleaved α_1-antitrypsin shows variability of the reactive center and other loops, J. Mol. Biol. 306 (2001) 109–119.

[7] M. Simonovic, P.G.W. Gettins, K. Volz, Crystal structure of human PEDF, a potent anti-angiogenic and neurite growth-promoting factor, Proc. Natl. Acad. Sci. 98 (2001) 11131–11135.

[8] P.E. Stein, A.G.W. Leslie, J.T. Finch, W.G. Turnell, P.J. McLaughlin, R.W. Carrel, Crystal structure of ovalbumin as a model for the reactive centre of serpins, Nature 347 (1990) 99–102.

[9] S.J. Harrop, L. Jankova, M. Coles, D. Jardine, J.S. Whittaker, A.R. Gould, A. Meister, G.C. King, B.C. Mabbutt, P.M.G. Curmi, The crystal structure of plasminogen activator inhibitor at 2.0 Å resolution: implications for serpin function, Structure 7 (1999) 43–54.

[10] A. Imberty, S. Pérez, Structure, conformation, and dynamics of bioactive oligosaccharides: theoretical approaches and experimental validations, Chem. Rev. 100 (2000) 4567–4588.

[11] W. Li, D.J.D. Johnson, C.T. Esmon, J.A. Huntington, Structure of the antithrombin–thrombin–heparin ternary complex reveals the antithrombotic mechanism of heparin, Nat. Struct. Biol. 11 (2004) 857–862.

[12] H. Verli, J.A. Guimarães, Molecular dynamics simulations of a decasaccharide fragment of heparin in aqueous solution, Carbohydr. Res. 339 (2004) 281–290.

[13] IUPAC-IUB Comission on Biochemical Nomenclature, Abbreviations and symbols for description of conformation of polypeptide chains, J. Mol. Biol. 52 (1970) 1–17.

[14] D.M.F. van Aalten, B. Bywater, J.B.C. Findlay, M. Hendlich, R.W.W. Hooft, G. Vriend, PRODRG, a program for generating molecular topologies and unique molecular descriptors from coordinates of small molecules, J. Comput. Aided Mol. Des. 10 (1996) 255–262. http://davapc1.bioch.dundee.ac.uk/programs/prodrg/prodrg.html.

[15] MOLDEN, Schaftenaar, G. 1997, CAOS/CAMM Center, University of Nijmegen, Toernooiveld 1, 6525 ED Nijmegen, The Netherlands.

[16] W. Humphrey, A. Dalke, K. Schulten, VMD—Visual Molecular Dynamics, J. Mol. Graphics 14 (1996) 33–38. http://www.ks.uiuc.edu/Research/vmd/.

[17] R. Koradi, M. Billeter, K. Wüthrich, MOLMOL: a program for display and analysis of macromolecular structures, J. Mol. Graphics 14 (1996) 51–55.

[18] N. Guex, M.C. Peitsch, Swiss-Model and the Swiss-Pdb Viewer: an environment for comparative protein modeling, Electrophoresis 18 (1997) 2714–2723. http://www.expasy.org/spdbv.

[19] H.J.C. Berendsen, D. van der Spoel, R. van Drunen, GROMACS—a message-passing parallel molecular-dynamics implementation, Comput. Phys. Commun. 91 (1995) 43–56.

[20] D. van der Spoel, E. Lindahl, B. Hess, A.R. van Buuren, E. Apol, P.J. Meulenhoff, D.P. Tieleman, A.L.T.M. Sijbers, K.A. Feenstra, R. van Drunen, H.J.C. Berendsen, GROMACS user manual version 3.2, Nijenborgh 4, 9747 AG Groningen, The Netherlands, 2004.

[21] L. Jin, J.P. Abrahams, R. Skinner, M. Petitou, R.N. Pike, R.W. Carrel, The anticoagulant activation of antithrombin by heparin, Proc. Natl. Acad. Sci. 94 (1997) 14683–14688.

[22] H.J.C. Berendsen, J.R. Grigera, T.P. Straatsma, The missing term in effective pair potentials, J. Phys. Chem. 91 (1987) 6269–6271.

[23] B.L. de Groot, H. Grubmüller, Water permeation across biological membranes: mechanism and dynamics of aquaporin-1 and GlpF, Science 294 (2001) 2353–2357.

[24] C.F. Becker, J.A. Guimarães, H. Verli, Molecular dynamics and atomic charge calculations in the study of heparin conformation in aqueous solution, Carbohydr. Res. 340 (2005) 1499–1507.

[25] B. Hess, H. Bekker, H.J.C. Berendsen, J.G.E.M. Fraaije, LINCS: a linear constraint solver for molecular simulations, J. Comput. Chem. 18 (1997) 1463–1472.

[26] S. Miyamoto, P.A. Kollman, SETTLE: an analytical version of the SHAKE and RATTLE algorithm for rigid water models, J. Comput. Chem. 13 (1992) 952–962.
[27] T. Darden, D. York, L. Pedersen, Particle Mesh Ewald—an *N* log (*N*) method for Ewald sums in large systems, J. Chem. Phys. 98 (1993) 10089–10092.
[28] H.J.C. Berendsen, J.P.M. Postma, A. DiNola, J.R. Haak, Molecular-dynamics with coupling to an external bath, J. Chem. Phys. 81 (1984) 3684–3690.
[29] M. Hricovíni, M. Guerrini, A. Bisio, G. Torri, M. Petitou, B. Casu, Conformation of heparin pentasaccharide bound to antithrombin III, Biochem. J. 359 (2001) 265–272.
[30] B. Mulloy, M.J. Forster, C. Jones, D.B. Davies, N.M.R. and molecular-modeling studies of the solution conformation of heparin, Biochem. J. 293 (1993) 849–858.
[31] A.C. Wallace, R.A. Laskowski, J.M. Thornton, LIGPLOT: a program to generate schematic diagrams of protein–ligand interactions, Protein Eng. 8 (1995) 127–134.
[32] V. Arocas, S.C. Bock, S.T. Olson, I. Björk, The role of Arg46 and Arg47 of antithrombin in heparin binding, Biochemistry 38 (1999) 10196–10204.
[33] S.J. Kridel, D.J. Knauer, Lysine residue 114 in human antithrombin III is required for heparin pentasaccharide-mediated activation, J. Biol. Chem. 272 (1997) 7656–7660.
[34] V. Arocas, S.C. Bock, S. Raja, S.T. Olson, I. Björk, Lysine 114 of antithrombin is of crucial importance for the affinity and kinetics of heparin pentasaccharide binding, J. Biol. Chem. 276 (2001) 43809–43817.
[35] S. Schedin-Weiss, U.R. Desai, S.C. Bock, P.G.W. Gettins, S.T. Olson, I. Björk, Importance of lysine 125 for heparin binding and activation of antithrombin, Biochemistry 41 (2002) 4779–4788.
[36] U. Desai, R. Swanson, S.C. Bock, I. Björk, S.T. Olson, Role of arginine 129 in heparin binding and activation of antithrombin, J. Biol. Chem. 275 (2000) 18976–18984.
[37] W.F. van Gunsteren, H.J.C. Berendsen, Computer simulations of molecular dynamics: methodology, applications, and perspectives in chemistry, Angew. Chem. Int. Ed. Engl. 29 (1990) 992–1023.
[38] M. Karplus, G.A. Petsko, Molecular dynamics simulations in biology, Nature 347 (1990) 631–639.
[39] R. Skinner, J.-P. Abrahams, J.C. Whisstock, A.M. Lesk, R.W. Carrel, M.R. Wardell, The 2.6 Å structure of antithrombin indicates a conformational change at the heparin binding site, J. Mol. Biol. 266 (1997) 601–609.
[40] P.R. Elliott, D.A. Lomas, R.W. Carrel, J.P. Abrahams, Inhibitory conformation of the reactive loop of alpha 1-antitrypsin, Nat. Struct. Biol. 3 (1996) 676–681.
[41] A. Futamura, J.M. Beechem, P.G.W. Gettins, Conformational equilibrium of the reactive center loop of antithrombin examined by steady state and time-resolved fluorescence measurements: consequences for the mechanism of factor Xa inhibition by antithrombin–heparin complexes, Biochemistry 40 (2001) 6680–6687.
[42] P.H. Lin, U. Sinha, A. Betz, Antithrombin binding of low molecular weight heparins and inhibition of factor Xa, Biochim. Biophys. Acta 1562 (2001) 105–113.
[43] R.F. Melo, M.S. Pereira, D. Foguel, P.A.S. Mourão, Antithrombin-mediated anticoagulant activity of sulfated polysaccharides, J. Biol. Chem. 279 (2004) 20824–20835.
[44] W. Kabsch, C. Sander, Dictionary of protein secondary structure: pattern-recognition of hydrogen-bonded and geometrical features, Biopolymers 22 (1983) 2577–2637.
[45] R.A. Laskowski, M.W. MacArthur, D.S. Moss, J.M. Thornton, PROCHECK: a program to check the stereochemical quality of protein structures, J. Appl. Crystallogr. 26 (1993) 283–291.
[46] C.A.A. van Boeckel, P.D.J. Grootenhuis, A. Visser, A mechanism for heparin-induced potentiation of antithrombin-III, Nat. Struct. Biol. 1 (1994) 423–425.
[47] S.T. Olson, I. Björk, R. Sheffer, P.A. Craig, J.D. Shore, J. Choay, Role of the antithrombin-binding pentasaccharide in heparin acceleration of antithrombin–proteinase reactions, J. Biol. Chem. 267 (1992) 12528–12538.
[48] R.S. de Witte, E.J. Shakhnovich, Pseudodihedrals: simplified protein backbone representation with knowledge-based energy, Protein Sci. 3 (1994) 1570–1581.
[49] J.D. Hirst, C.L. Brooks III, Helicity, circular dichroism and molecular dynamics of proteins, J. Mol. Biol. 243 (1994) 173–178.